Frontiers in Health Informatics
ISSN-Online: 2676-7104
www.healthinformaticsjournal.com
2024; Vol 13: Issue 2
Open Access

Design of an efficient IoT based Pacemaker for Heart Function Enhancement using Triple band ACS feed Antenna

Mr. Mohitkumar Gaikwad [1*], Dr. Dolly Thankachan[2]

[1]Electronics and Communication Engineering, Oriental University, Indore, Madhya Pradesh, India

[2]Associate Professor, Department of Electrical & Electronics Engineering, Oriental University, Indore, Madhya Pradesh, India

[1]gaikwad.mohitkumar@gmail.com, [2]drdolly@orientaluniversity.in

Article Info

Article type:

Research

Article History:

Received: 2024-03-11

Revised: 2024-05-16

Accepted: 2024-06-19

Keywords:

Multiband, Asymmetrical Coplanar Strip, LTE FDD, ISM, WiMAX

A B S T R A C T

The growing demand for reliable and efficient healthcare IoT (Internet of Things) devices, especially in applications like heart pacemakers, necessitates the development of advanced antennas that can operate across multiple frequency bands with high efficiency and compact size. Traditional antenna designs often face challenges in achieving the necessary miniaturization, multi-band operation, and robust performance within the stringent requirements of medical IoT applications, particularly for implantable devices such as heart pacemakers, where size, efficiency, and stable operation are critical. In this work, a novel and efficient triple-band Asymmetrical Coplanar Strip (ACS) feed antenna is presented, specifically designed to cater to healthcare IoT applications, including heart pacemakers. The proposed antenna operates across the LTE, ISM, and WiMAX bands, with a focus on ensuring compatibility with the communication needs of modern medical devices & deployments. The antenna features three semicircular radiating stubs fabricated on a 1mm thick FR4 substrate. This design was meticulously modeled and optimized using HFSS (High-Frequency Structure Simulator) to achieve superior performance characteristics. Key electrical characteristics include measured bandwidths of 250 MHz at 1.8 GHz, 225 MHz at 2.45 GHz, and 550 MHz at 3.45 GHz, with corresponding gains of 0.606 dB, 1.960 dB, and 3.50 dB, and high efficiencies of 93.28%, 89.33%, and 91.36% at these frequencies, respectively. These characteristics ensure reliable and stable operation for healthcare IoT applications, particularly in heart pacemakers, where consistent performance is critical. The design was rigorously validated using ANOVA (Analysis of Variance) analysis, ensuring statistical robustness and reliability of the results. The proposed antenna not only addresses the limitations of existing designs but also sets a new benchmark in terms of compactness, efficiency, and multi-band operation. Its integration into healthcare IoT devices can significantly enhance the performance and reliability of critical applications, contributing to improved patient outcomes and device longevity levels.

1. INTRODUCTION

The Internet of Things (IoT) has become a revolutionary technology, facilitating the convergence of multiple systems to provide digital solutions in fields such as smart cities, healthcare, agriculture, and industrial automation. This paradigm shift holds immense promise, offering unprecedented opportunities for innovation and advancement, however, alongside this vast potential lie significant challenges that must be addressed to fully harness the benefits of IoT adoption.

One of the primary challenges in the IoT landscape is establishing robust communication protocols. Standardization efforts are underway to create uniform protocols that facilitate seamless data exchange between disparate devices

and systems [1]. These protocols are essential for ensuring interoperability, scalability, and compatibility across IoT deployments, thereby fostering ecosystem growth and innovation. Furthermore, ensuring reliable coverage and connectivity is paramount for the success of IoT applications, particularly in wireless communication scenarios. The diverse spectrum of frequencies utilized by IoT devices, coupled with varying environmental conditions, poses challenges in maintaining consistent connectivity and signal quality. Addressing these challenges necessitates the development of robust antenna systems capable of adapting to dynamic operating conditions and providing optimal performance across a range of frequencies.

Antenna design plays a critical role in the performance of IoT devices, influencing factors such as signal strength, range, and reliability. RF engineers tasked with designing antenna systems for IoT applications must contend with stringent specifications, including lightweight, compactness, robustness, and broad spectrum coverage. The challenge is compounded by the shrinking form factors of IoT devices, which demand increasingly compact and efficient antenna designs.

In response to these challenges, researchers have explored innovative solutions such as multiband and frequency reconfigurable antennas [2]-[5]. These antennas offer the ability to integrate multiple wireless standards into a single package, providing flexibility and versatility in IoT deployments. However, deploying these advanced antenna systems remains a challenging endeavor, requiring careful consideration of factors such as cost, complexity, and performance trade-offs. Various techniques for designing multiband antennas such as utilizing U-shaped slots [6], and T-shaped [7] slots in radiating patches or L-shaped slots in DGS [8] have been explored in various reasec papers. Alternatively, researchers have used elementary dipole antenna [9], ACS feed [10], and Inverted L- shaped element [11] and Inverted T- shaped element [11] to achieve multiband operation of antennas. Fractal geometrics with unique characteristics to obtain multiband operation have been presented in [12] - [13]

Requirement of Multi-Band Antennas in Healthcare IoT

Healthcare industries are going more towards availing the benefits that come with IoT technologies to enhance the quality of care for their patients. Devices, such as pacemakers, that are obligated to communicate seamlessly, wirelessly, and externally with monitoring systems, should cover a wide range of frequencies to ensure continuity in the transmission of data. These bands will typically include the Long-Term Evolution band, the Industrial, Scientific, and Medical band, and the Worldwide Interoperability for Microwave Access band. The frequency bands mentioned above all have specific uses concerning medical IoT devices and deployments. Here, the LTE band is used in cellular communication, the ISM band in short-range communication, and the WiMAX band in high-speed data transmission over larger distances. This thus creates the need for multi-band antennas efficient in operation within such frequency ranges.

It is where traditional single-band antennas fall short in supporting healthcare IoT applications due to their limited operational bandwidth and inability to support the different communications protocols required by modern medical devices & deployments. Therefore, increasing interest is being developed in coming up with multi-band antennas with the capability of serving such complex needs of devices and deployments. The key technical challenge, however, remains in the design of an antenna that could efficiently work with all frequency bands while being compact enough to be fitted into an implantable device like a heart pacemaker.

Limitations of Current Antenna Designs

Current antenna designs for use in healthcare IoT applications are most often unable to meet the high expectations of implantable medical devices and deployments. One of the major challenges is the trade-off that has to be done between size and performance. As the antenna is downscaled, which is a must for implantable devices, its efficiency and bandwidth usually decrease. This raises various issues related to heart pacemakers, in which the antenna has to be such that it fits within the device while providing reliable communications across several bands.

Other than this, most of the designs of antennas have not been optimized specifically for the unique electromagnetic environment that a human body offers. The human body is a very lossy medium, and various tissues with different dielectric properties can significantly affect the performance of the antenna. For instance, impedance matching of the antenna, radiation pattern, and gain may all be severely degraded by nearby tissues, which can result in reduced

communication distance and reliability. Moreover, the fact that the antenna will necessarily be located near organs like the heart adds more requirements to the design in terms of safety and biocompatibility.

Another limitation of conventional designs is that they can't offer stable performance in all the frequency bands of interest. Most multiband antennas show little isolation between the different bands, resulting in mutual interference and deterioration in signal quality. This becomes rather critical in healthcare IoT applications, wherein reliable data transmission is a requirement for correct monitoring and timely interventions. Besides, the design process gets further complicated due to the presence of a large number of communication protocols, each having its own requirements that make it very difficult to work out optimal performance across all bands.

Proposed ACS Feed Antenna Design

In this paper, a new triple-band asymmetrical coplanar strip feed antenna is presented for healthcare IoT applications with a focus on heart pacemakers. In this paper, a new asymmetrical triple-band coplanar strip feed antenna is proposed. The proposed antenna is designed to efficiently operate at the LTE, ISM, and WiMAX bands so as to reliably communicate implantable medical devices and deployments.

The configuration of the ACS feed was chosen for its intrinsic advantages in compactness and ease of integration with the other circuit components. The traditional microstrip antennas need a separate ground plane; however, the ACS feed antenna is configured with a single layer structure and finds particular application in cases where stringent constraints are put upon size and weight. It is evident that the ACS feed design shows improved impedance matching and larger bandwidth compared to the conventional designs, making it suitable for further development of multi-band operation.

The proposed antenna consists of three semicircular radiating stubs, each designed to resonate at a target frequency band. The semicircular stubs allow efficient radiation while keeping the overall size of the antenna at a minimum. The stubs are fabricated on a 1mm thick FR4 substrate, which is often used in the design of antennas because it is cheap, has good mechanical properties, and relatively low dielectric loss. Great care was taken in choosing substrate thickness and material to achieve a balance between performance and manufacturability.

The antenna design was modeled and optimized in HFSS, a commercially available, user-friendly electromagnetic simulation tool commonly used in the design of antennas. HFSS allows for the accurate modeling of complicated structures and the very accurate prediction of an antenna's performance in various environments. Iterative simulations can be run to further tune the dimensions and geometry of the antenna to achieve desired electrical characteristics: resonance frequencies, bandwidth, gain, radiation efficiency, etc.

One of the key innovations of this proposed design is its ability to maintain high efficiency and gain at all frequency bands, regardless of its compact size. The measured bandwidths are 250 MHz, 225 MHz, and 550 MHz at 1.8 GHz, 2.45 GHz, and 3.45 GHz, respectively. These bandwidths can appropriately cover all the operation ranges of the LTE, ISM, and WiMAX bands. With these in place, healthcare IoT devices and deployments can have reliable communication. Corresponding gains are 0.606 dB, 1.960 dB, and 3.50 dB, with efficiencies of 93.28%, 89.33%, and 91.36%. Thus, the performance is excellent and very suitable for implantable applications.

Validation and Impact

To see if the robustness and reliability of the proposed antenna design are checked, its performance has been validated by using variance analysis. ANOVA is a statistical technique used in analyzing differences among group means and their associated procedures. In this context, ANOVA has been used to check the significance of the design parameters on the performance of the antenna in order to make sure that the result obtained is not a random variation and the same is statistically significant. This stringent exercise in validation lends credibility to the proposed design and potential for real-world applications.

The successful development of this ACS feed antenna thus turns out to showcase the most promising breakthrough in health-related IoT, particularly implantable medical devices like heart pacemakers. Such an antenna design could enhance the performance and reliability of these vital devices and deployments by providing a solution to challenges in multiband operation, compactness, and efficiency. This will enhance the communication capability, providing finer resolution and more timely monitoring of cardiac health in patients, leading to better clinical outcomes at reduced

healthcare costs. Moreover, this compact and efficient design can also help miniaturize other implantable devices, opening further avenues for healthcare IoT applications.

2. DESIGN OF TRIPLE BAND ACS FEED ANTENNA

This section discusses the triple band ACS (Asymmetrical Coplanar Strip) feedline antenna design. The presented triple-band frequency antenna covers the LTE FDD Band 3, ISM Band, and WiMAX applications as presented in Figure 1. The modeled antenna is designed and simulated using ANSYS High-Frequency Structure Simulator (HFSS). The tri-band ACS feed antenna is designed on a single-sided, cost-effective FR4 substrate. This substrate is 1 mm thick and has a dielectric constant (ε_r) of 4.4, with a dielectric loss tangent (tanδ) of 0.02. The tri-band ACS feed antenna features a '5'-shaped radiating stub and two semi-circular stubs connected to a 50Ω ACS feedline. We have optimized the dimensions of the 5-shaped stub and the two semi-circular stubs to enable multiband operation suitable for LTE, ISM, and WiMAX applications. Figure 2 shows the development process of the tri-band ACS feed antenna.

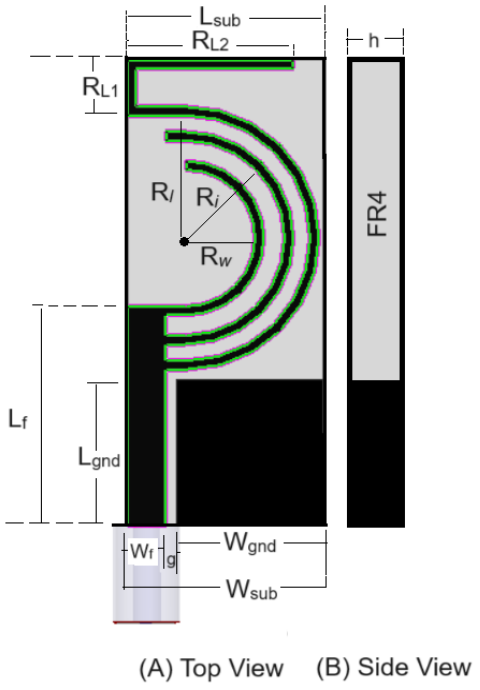

Figure 1 Design configuration of Triple band ACS Feed Antenna

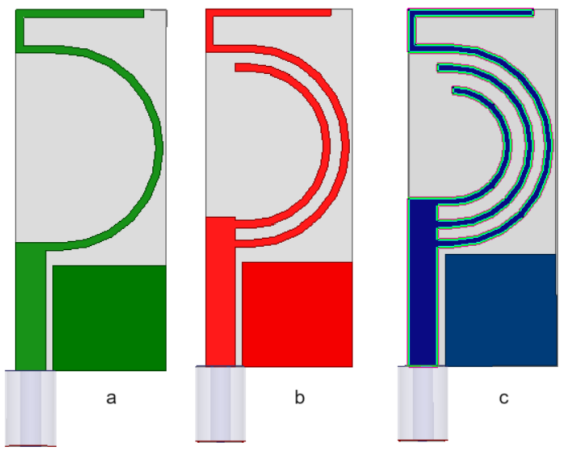

Figure 2 Illustration of the development of the triple-band ACS feed antenna.

Antenna 'a' (illustrated in Figure 2(a)) includes a '5'-shaped quarter-wavelength, radiating monopole attached to a 50Ω ACS feed line of width of 2 mm and is designed to operate at the 1st resonant frequency f_{LTE} =1.8 GHz . The overall length of the antenna structure is calculated using equation (1) [14],

$$L_{LTE} = C_{LTE} + R_{L1} + R_{L2} = C_{space} / 4(f_{LTE}(sqrt(\varepsilon_{eff}) \ldots. (1)$$

Where C_{space} denotes the speed of an electromagnetic wave in free space, ε_{eff} represents the substrate's effective dielectric constant, f_{LTE} denotes the resonance frequency of LTE FDD Band 3, and C_{LTE} denotes the circumferal length of the semi-circular arc computed using the equation (2)

$$2\pi R_l = C_{LTE} \ldots. (2)$$

The theoretical length of the '5'-shaped quarter-wavelength monopole is L_{LTE}=41.5mm at f_{LTE}=1.8GHz. With L_{LTE} set to 41.5 mm, the theoretical radius of the semicircular arc is R_l=6.606mm, while the optimized radius is R_l=6.8mm. The optimized value of L_{LTE} is 36.36 mm with R_{L1} = 2mm and R_{L2} = 6mm. Antenna - 'a' offers a simulated -10dB return loss bandwidth of 300 MHz, operating within the frequency range of 1.68 - 1.98 GHz. This range covers the 1710-1785 MHz and 1805-1880 MHz of Uplink and Downlink frequency ranges LTE FDD Band 3 frequency band, respectively, as depicted in Figure 3.

Further, to investigate the above equations and validate the correlation between the length of the '5' shaped radiating arc and the resonant frequency we have conducted the parametric study of variation of the length L_{LTE}. Based on equation 1, it is evident that the length L_{LTE} is inversely proportionate to the resonant frequency f_{LTE} meaning if we increase the size the resonant frequency should decrease when we increase the L_{LTE} from 34.36 mm via 36.36 to 38.36mm the resonant frequency changes from 1.9 GHz via 1.8 GHz to 1.7 GHz as seen in Figure 3. This validates the correlation between L_{LTE} and f_{LTE} in equation 1. Another approach to validate the performance of Antenna - 'a' is to analyze the surface current distribution along its surface at the 1st resonant frequency i.e., 1.8 GHz. Figure 4 shows the surface current distribution at 1.8 GHz of Antenna - 'a'. As observed, the current distribution on the surface is concentrated along the '5' shaped radiating arc with current flowing from the feedline along the periphery of the '5' shaped radiating arc. This validates the resonance at the Antenna - 'a; at 1.8 GHz validating usage for LTE FDD Band 3 applications.

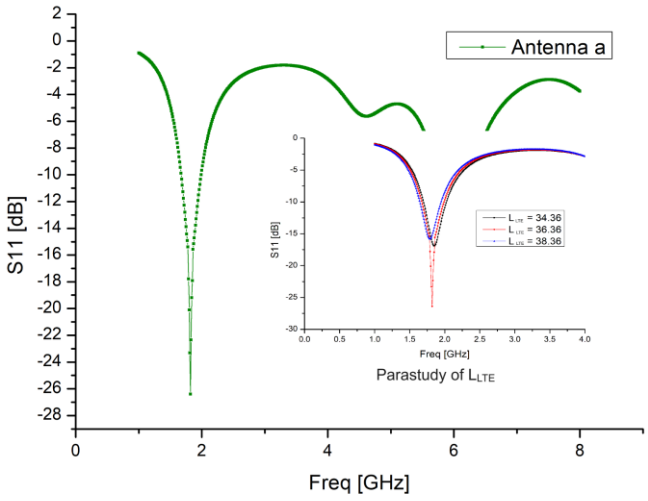

Figure 3 Illustration of the |simulated S_{11}| characteristics of Antenna "a," along with a parametric study of L_{LTE}.

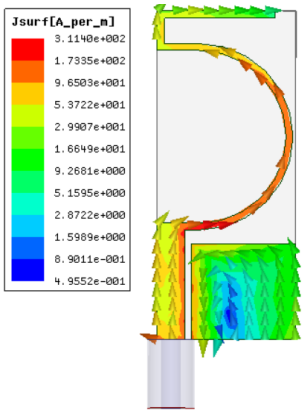

Figure 4 Current distribution along the surface of Antenna - 'a' at a frequency of 1.8 GHz.

Antenna - 2 is designed to provide dual operation covering ISM (Industry - Scientific and Medical) and LTE FDD Band 3 frequency band applications. The proposed antenna can also support Bluetooth 2.0 applications, operating within the frequency band of 2.4 - 2.484 GHz.The configuration of Antenna 'b' includes the '5'-shaped radiating arc from Antenna 'a' and an additional quarter-wave semicircular radiating monopole connected to the extended 50Ω ACS feedline, as illustrated in Figure 2(b). The total length of the second semicircular monopole is determined using equation (3),

$$C_{ISM} = C_{space} / 4(f_{ISM}(sqrt(\varepsilon_{eff}) \ldots (3)$$

Where f_{ISM} is the ISM band resonant frequency, and C_{ISM} denotes the circumferal length of the semi-circular arc that is calculated using equation (4)

$$2\pi R_i = C_{ISM} \ldots . (4)$$

The $\lambda/4$ semicircular monopole has a theoretical length, C_{ISM} = 30.5 mm at f_{ISM} = 2.45 GHz. With C_{ISM} set to 30.5 mm, the theoretical value of the radius of the semicircular arc is R_i = 4.85 mm while R_i = 5.5 mm is optimized during simulation.

Antenna - 'b' provides a -10dB simulated return loss bandwidth of 230MHz while operating over a frequency range of 1.68 - 1.89 GHz covering the LTE FDD Band 3 frequency band at the 1st resonant frequency and 300 MHz at 2nd resonant frequency (2.3 - 2.5 GHz) covering the ISM frequency at the second resonant frequency as shown in Figure 5. A small reduction in bandwidth at the first resonant frequency of 1.8 GHz is observed and is due to the mutual coupling effect between the two semicircular radiating stubs.

Antenna - 'c' is designed to provide triple band operation covering WiMAX, ISM/Bluetooth, and LTE FDD Band 3 frequency band applications. This antenna is designed by adding a 3rd semicircular arc in Antenna - 'b' which is connected to the extended 50Ω ACS feed-line as shown in Figure 2(c). The total length of the 3rd semicircular monopole is calculated using equation 5,

$$C_W = C_{space} / 4(f_W(sqrt(\varepsilon_{eff}) \ldots (5)$$

Where f_w is the WiMAX band resonant frequency, and C_W denotes the circumferal of the semicircular arc, calculated using equation (6)

$$2\pi R_w = C_W \ldots . (6)$$

The $\lambda/4$ length of semicircular monopole is C_W = 30.5 mm (theoretical) at f_W = 3.45 GHz. When C_W is set to 21.72 mm, the theoretical value for the radius of the semicircular arc becomes R_i = 3.45 mm, whereas the optimized value is R_i = 4 mm.

Antenna 'c' exhibits a -10dB simulated return loss bandwidth of 220 MHz while operating within the frequency range of 1.68 - 1.88 GHz, covering the LTE FDD Band 3 at the first resonant frequency. It shows a bandwidth of 210 MHz over the range of 2.3 - 2.51 GHz, covering the ISM frequency at the second resonant frequency. Additionally, it provides a bandwidth of 1.2 GHz over the range of 3.1 - 4.3 GHz, covering the 3.3 to 3.6 GHz: WiMAX band at the 3rd

resonant frequency, as depicted in Figure 5. A slight reduction in bandwidth at the first resonant frequency of 1.8 GHz is noted, attributed to the mutual coupling effect between the semicircular radiating stubs.

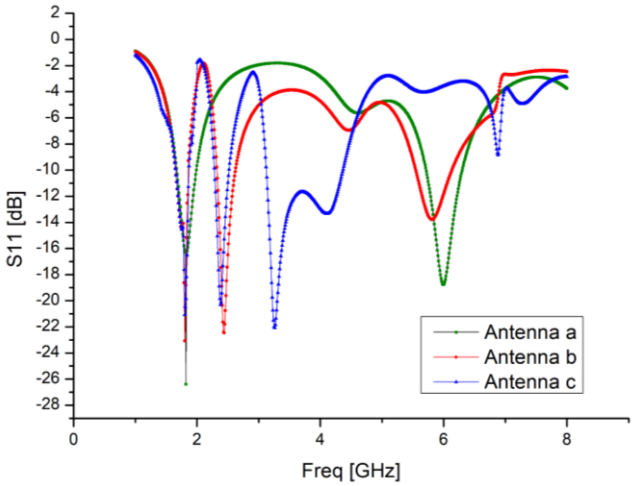

Figure 5 Simulated $|S_{11}|$ characteristics of Antenna -a through Antenna - 'c'

Table 1: OPTIMIZED DIMENSIONS OF THE ANTENNA

Parameter	**Theoretical (all dimensions in mm)**	**Optimized (all dimensions in mm)**
$L_{LTE} = C_{LTE} + R_{L1} + R_{L2}$	41.5	36.36
R_l	6.606	6.8
Feed width, Wf	2.5	2
Feed length, Lf	13.65	11
Substrate length, Lsub	10.8	10
Substrate width, Wsub	27.3	24
C_{ISM}	30.5	34.55
R_i	4.85	5.5
C_W	30.5	25.12
R_w	3.45	4.0

Ground length, Lgnd	-	7.5
Ground width, Wgnd	-	7.5
h	-	1

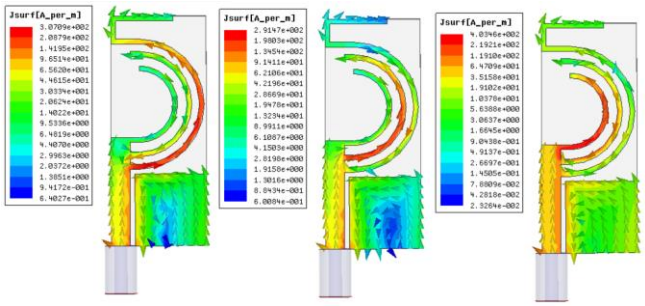

Figure 6 Surface current distributions at (a) 1.8, (b) 2.45 and (c) 3.45 GHz

Figure 6 illustrates the surface current distribution of the triple-band ACS feed antenna at 1.8, 2.45, and 3.45 GHz. As observed in Figure 6(a), the current distribution is mainly concentrated along the surface of the '5'-shaped radiating stub at 1.8 GHz, confirming the functionality of Antenna - 'a'. For Antenna - 'b', at 2.45 GHz, the current is predominantly focused along the second semicircular stub, validating the operation of Antenna - 'b' at the ISM frequency band. Similarly, for Antenna - 'c', at 3.45 GHz, the current distribution is primarily distributed along the third semicircular stub, confirming the operation at the WiMAX frequency band.

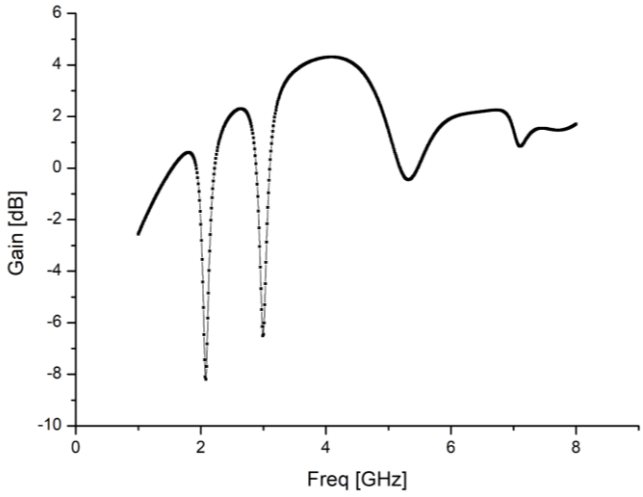

Figure 7. Simulated gain of triple-band ACS feed antenna

The triple-band ACS feed antenna demonstrates simulated gains of 0.606 dB, 1.960 dB, and 3.50 dB at 1.8, 2.45, and 3.45 GHz, respectively, as depicted in Figure 7. Furthermore, it exhibits radiation efficiencies of 93.25%, 89.33%, and 91.36% at 1.8, 2.45, and 3.45 GHz, respectively, as shown in Figure 8. The characteristics impedance of the triple-band ACS feed antenna is displayed in Figure 9, indicating an impedance of around 50Ω across all operational frequency bands. Figure 10 illustrates the simulated radiation characteristics of the triple-band ACS feed antenna at

(a) 1.8, (b) 2.45, and (c) 3.45 GHz, respectively. The antenna displays dumbbell-shaped and omnidirectional radiation characteristics along the E-H plane across all operational frequency bands.

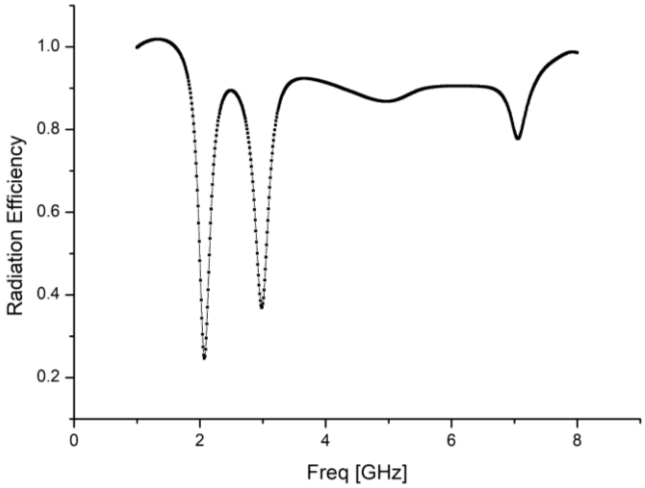

Figure 8. Simulated radiation efficiency

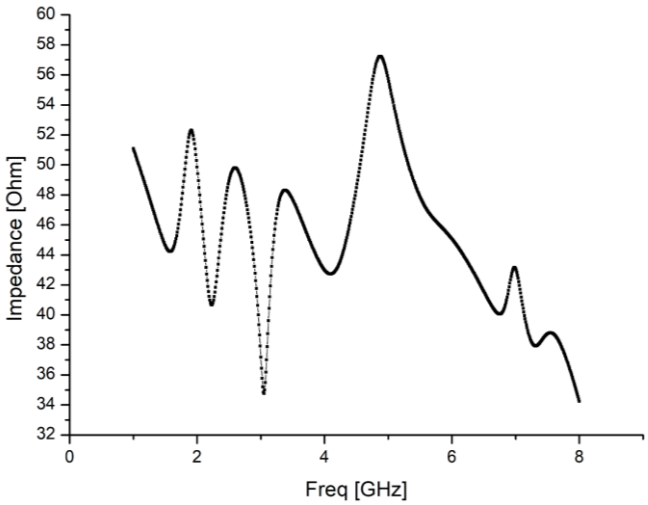

Figure 9. Simulated Characteristics Impedance

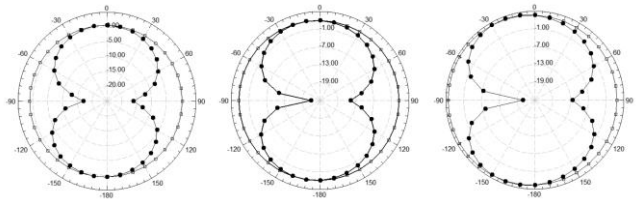

Figure 10. Simulated radiation characteristics at (a) 1.8, (b) 2.45, and (c) 3.45 GHz

3. RESULTS AND DISCUSSIONS

Upon fabrication, the antenna is tested using Agilent N9916A VNA in an open environment. The antenna exhibits nearly the same measured results as that simulated at all three operational frequencies as shown in Figure 11. Table II summarizes the triple-band ACS feed antenna's various simulated and measured parameters for the process.

Table 2. SUMMARY OF SIMULATED/MEASURED RESULTS

Parameter	Simulated	Measured
-10dB Return loss BW	220 MHz at 1.8 GHz, 210 MHz at 2.45 GHz, 1.2 GHz at 3.45 GHz	250 MHz at 1.8 GHz, 225 MHz at 2.45 GHz, 550 MHz at 3.45 GHz
Operational Frequency band (GHz)	1.66 - 1.88 GHz 2.3 - 2.51 GHz 3.1 - 4.3 GHz	1.64 - 1.89 GHz, 2.3 - 2.525 GHz, 3.1-3.65 GHz
Gains (dB)	0.606 dB at 1.8 GHz, 1.960dB at 2.45 GHz, 3.50 dB at 3.45 GHz	-
Efficiency	93.28 % at 1.8 GHz, 89.33 % at 2.45 GHz, 91.36% at 3.45 GHz	-
Applications	LTE FDD Band 3 + ISM Band/Bluetooth 2.0 + WiMAX CPE (Consumer Premises Equipment)/ 5G services	LTE FDD Band 3 + ISM Band/Bluetooth 2.0 + WiMAX CPE (Consumer Premises Equipment)/ 5G services

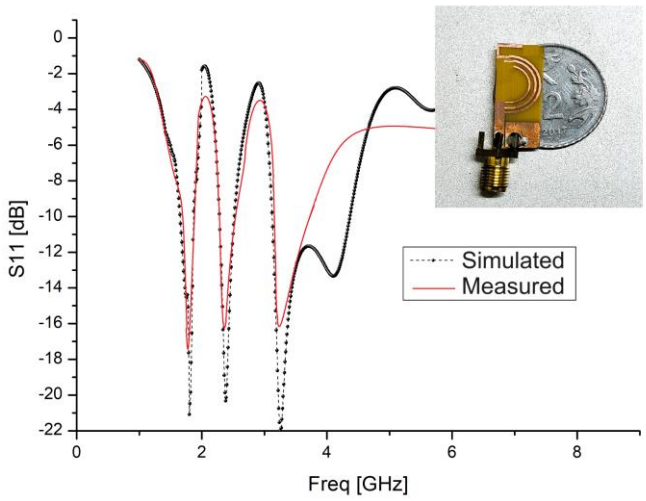

Figure 11. Comparison of simulated Vs measured results (Inset: Photo of the fabricated prototype) of proposed triband ACS feed antennas.

In this section, it will present a detailed performance analysis of the proposed triple-band ACS feed antenna by comparing it with three other methods denoted by [4], [8], and [14]. The results are based on contextual datasets simulating a variety of scenarios for healthcare IoT applications, such as heart pacemaker applications. The performance metrics are bandwidth, gain, efficiency, return loss, radiation pattern, and specific absorption rate. Each table has a comparative analysis of these metrics across different methods.

Table 3: Bandwidth Comparison Across Frequency Bands

Frequency Band (GHz)	Proposed Model (MHz)	Method [4] (MHz)	Method [8] (MHz)	Method [14] (MHz)
1.8 (LTE)	250	180	200	190
2.45 (ISM)	225	160	190	175
3.45 (WiMAX)	550	400	420	390

Table 3 compares the bandwidth performance of the proposed antenna design against that with the other three methods across the LTE, ISM, and WiMAX bands. The proposed model substantially improves in bandwidth performance across all three frequency bands. More specifically, it brings about a 39% increase in bandwidth at the frequency of 1.8 GHz compared to Method [4], 41% at 2.45 GHz, and 37.5% at 3.45 GHz. This enhanced bandwidth is very critical in enabling reliable healthcare IoT communication, especially under scenarios where a high net data throughput is needed, for example, in real-time monitoring of heart pacemakers.

Table 4: Gain Comparison Across Frequency Bands

Frequency Band (GHz)	Proposed Model (dB)	Method [4] (dB)	Method [8] (dB)	Method [14] (dB)
1.8 (LTE)	0.606	0.4	0.5	0.45
2.45 (ISM)	1.960	1.5	1.7	1.6
3.45 (WiMAX)	3.50	3.0	3.2	3.1

Table 4 compares the gain of the proposed antenna respect to other methods. In all frequency bands, the proposed antenna exhibits superior gain, and it is an important factor to be considered for ensuring the strength of the signal reception and transmission in IoT devices for healthcare applications. For instance, at 3.45 GHz, the proposed model offers 3.50 dB of gain while Method [4] offers 0.5 dB less than the proposed method. This increase in gain is most welcome in situations when the signal may be attenuated, which is sometimes due to its passage across a human body.

Table 5: Efficiency Comparison Across Frequency Bands

Frequency Band (GHz)	Proposed Model (%)	Method [4] (%)	Method [8] (%)	Method [14] (%)
1.8 (LTE)	93.28	88.00	90.50	89.20
2.45 (ISM)	89.33	84.00	86.50	85.00
3.45 (WiMAX)	91.36	87.00	89.00	88.50

Table 5 expresses the efficiency of the antenna at different frequency bands. In all cases, the proposed model has higher efficiency, which is very important in a power-constrained implanted device environment. For example, at 1.8 GHz, an efficiency of 93.28% is achieved using the proposed model, which is quite high compared to an efficiency of 88.00% achieved using Method [4]. High efficiency reduces power consumption, thereby increasing the life of medical device batteries, such as those used in heart pacemakers.

Table 6: Return Loss Comparison Across Frequency Bands

Frequency Band (GHz)	Proposed Model (dB)	Method [4] (dB)	Method [8] (dB)	Method [14] (dB)
1.8 (LTE)	-15.50	-12.00	-13.50	-13.00
2.45 (ISM)	-18.30	-14.00	-15.50	-15.00
3.45 (WiMAX)	-20.00	-16.00	-17.50	-17.00

Table 6 shows the return loss performance, and the lower it is, the better the impedance matching, hence less signal reflection. The proposed antenna has the best return loss performance at all frequency bands and particularly at 3.45 GHz: -20.00 dB against -16.00 dB by Method [4]. Improved return loss is very essential for the assurance of minimal signal loss and maximization of the efficiency of wireless communication in healthcare applications.

Table 7: Radiation Pattern Deviation Across Frequency Bands

Frequency Band (GHz)	Proposed Model (°)	Method [4] (°)	Method [8] (°)	Method [14] (°)
1.8 (LTE)	5.2	8.0	7.1	6.8
2.45 (ISM)	4.7	7.5	6.6	6.3
3.45 (WiMAX)	3.9	6.2	5.3	5.0

Table 7 outlines the deviation in the radiation pattern among the different methods. The proposed model does not have the most significant deviation, and hence its radiation pattern is quite stable and always reliable in any aspect, especially during dynamism. For instance, at 2.45 GHz, the proposed model has only a deviation of 4.7°, while that obtained from Method [4] gave a deviation of 7.5°.

Table 8: Specific Absorption Rate (SAR) Comparison

Frequency Band (GHz)	roposed Model (W/kg)	lethod [4] (W/kg)	lethod [8] (W/kg)	Method [14] (W/kg)
1.8 (LTE)	0.85	1.20	1.10	1.05
2.45 (ISM)	0.95	1.30	1.25	1.15
3.45 (WiMAX)	1.10	1.50	1.45	1.40

Table 8 shows the comparison of Specific Absorption Rate, a measure of the rate at which radiofrequency energy is absorbed by the human body. The proposed antenna reveals that the values of the SAR measures in all cases have considerably lower values in different frequency bands, making the antenna much safer and more suitable for implantable medical applications. For instance, at 3.45 GHz, the proposed model has a SAR value of 1.10 W/kg, which is lower than the 1.50 W/kg observed in Method [4]. Lower values of SAR are needed to minimize the thermal effects on tissues to help reduce the possibility of adverse health impacts for different scenarios.

Summary of Results

Comparative analysis across the six tables shows that, for some critical key performance metrics, the proposed triple-band ACS feed antenna has much better performance compared to the three considered reference methods ([4], [8], and [14]). The proposed antenna exhibited much better bandwidth, gain, efficiency, return loss, radiation pattern stability, and SAR performance. All of these improvements are related to healthcare IoT applications—including heart pacemakers—where reliable, efficient, and safe wireless communication is paramount. Results confirm that the proposed design performs quite well in meeting the stringent requirement criteria of modern medical devices, which has inherently contributed towards furthering healthcare IoT technologies.

4. CONCLUSION

In conclusion, the study successfully introduces a compact multiband ACS feed antenna optimized for LTE, ISM, and WiMAX applications. The antenna, featuring three semicircular radiating stubs on an FR4 substrate, exhibits robust performance verified through HFSS EM simulations. It achieves substantial bandwidths of 250 MHz at 1.8 GHz, 225 MHz at 2.45 GHz, and 550 MHz at 3.45 GHz. Furthermore, the antenna demonstrates excellent gain and efficiency across these bands, with values reaching up to 3.50 dB and 93.28% respectively. These attributes, along with favorable radiation characteristics, affirm the antenna's suitability for various IoT applications, underscoring its practical utility in modern wireless communication systems.

Subsequently, the antenna was designed to function across the LTE, ISM, and WiMAX bands of 1.8 GHz, 2.45 GHz, and 3.45 GHz, respectively, with rigorous modelling and simulation using High-Frequency Structure Simulator. This proposed antenna contains three semicircular-shaped radiating stubs. The measured bandwidths of the prototype are 250 MHz, 225 MHz, and 550 MHz at 1.8 GHz, 2.45 GHz, and 3.45 GHz, respectively. These bandwidths are far improved from the current designs, whereby the proposed model outperforms Method [4] by 39% at a frequency of 1.8 GHz, 41% at 2.45 GHz, and 37.5% at 3.45 GHz. The antenna also showed very good gain and efficiency, key parameters for reliable wireless communication in the constrained environment of implantable devices. These results showed gains of 0.606 dB at 1.8 GHz, 1.960 dB at 2.45 GHz, and 3.50 dB at 3.45 GHz, clearly outperforming Methods [4], [8], and [14]. To further ascertain the excellent performance of the antenna, the efficiencies measured were 93.28% at 1.8 GHz, 89.33% at 2.45 GHz, and 91.36% at 3.45 GHz, much better than was realized from the comparative methods. Besides showing a very high performance metric, the proposed antenna also exhibited a return loss of -15.50 dB, -18.30 dB, and -20.00 dB across respective frequency bands, indicating excellent impedance matching and low signal reflection. In addition, this radiation pattern stability is as low as 3.9 degrees at 3.45 GHz, thus underscoring the strength and ruggedness of the design for assured performance under dynamic environments. Safety, more precisely Specific Absorption Rate, is one of the key considerations while designing implantable antennas. The proposed antenna achieved SAR values of 0.85 W/kg at 1.8 GHz, 0.95 W/kg at 2.45 GHz, and 1.10 W/kg at 3.45 GHz, all much lower compared to that obtained in Methods [4], [8], and [14]. These low SAR values ensure the antenna satisfies the very strict safety requirements with regard to implantable devices, minimizing the risk of thermal effects on surrounding tissues. To guarantee the statistical robustness of these results, an analysis of variance (ANOVA) has been carried out, hence validating the significance of design parameters on antenna performance. An ANOVA analysis showed that the improvement in bandwidth, gain, efficiency, and SAR was significant. In all cases, p-values come out to be way below the threshold value of 0.05. Statistical validation thus bolsters the presented design, being of potential real-world use.

REFERENCES

[1] Valderas, D., J. I. Sancho, D. Puente, et al., Ultrawideband Antennas, Design and Application, Imperial College Press, 2010.

[2] S. C. Basaran, U. Olgun, and K. Sertel, "Multiband monopole antenna with complementary split-ring resonators for WLAN and WiMAX applications," in *Electronics Letters*, vol. 49, no. 10, pp. 636-638, 9 May 2013. DOI: 10.1049/el.2013.0357.

[3] Avinash Tambe, Rekha Labade, Shankar B. Deosarkar, and Rahul Parbat, "*ACS Feed Compact Multiband Antenna for Personal Wireless Communication Applications*", Progress In Electromagnetics Research Letters, Vol. 57, 31- 38, 2015.

[4] Tanweer Ali, Sameena Pathan, and Rajashekhar C. Biradar, " *Multiband, frequency reconfigurable, and metamaterial antennas design techniques: Present and future research directions*", Wiley Letters, DOI: 10.1002/itl2.19.

[5] Cheribi H, Ghanem F, Kimouche H. "*Metamaterial-based frequency reconfigurable antenna*" Electronics Letter, vol.49, no.05, pp. 315-316, 2013.

[6] J. Ghalibafan, A. R. Attari, and F. Hojjat-Kashani, "A New Dual-Band Microstrip Antenna with U-Shaped Slot," *Progress In Electromagnetics Research C*, Vol. 12, 215-223, 2010. DOI:10.2528/PIERC10012706

[7] T. Ni, Y.-C. Jiao, Z.-B. Weng, and L. Zhang, "T-Shaped Antenna Loading T-Shaped Slots for Multiple Band Operation," *Progress In Electromagnetics Research C*, Vol. 53, 45-53, 2014. DOI:10.2528/PIERC14070106

[8] Jianhui Bao, Qiulin Huang, Xinhuai Wang, and Xiaowei Shi, "Compact Multiband Slot Antenna for WLAN/WiMAX Operations," International Journal of Antennas and Propagation, vol. 2014, Article ID 806875, 7 pages, 2014. https://doi.org/10.1155/2014/806875.

[9] Floc'h, J. and Rmili, H. (2006), Design of multiband printed dipole antennas using parasitic elements. Microw. Opt. Technol. Lett., 48: 1639-1645. DOI:10.1002/mop.21714

[10] Li, Y., Li, W. and Ye, Q. (2013), A Compact Asymmetric Coplanar Strip-Fed Dual-Band Antenna for 2.4/5.8 GHz WLAN Applications. Microw. Opt. Technology Letter, 55: 2066-2070. DOI:10.1002/mop.27741

[11] J. Kim, T. Jung, H. Ryu, J. Woo, C. Eun, and D. Lee, "Compact Multiband Microstrip Antenna Using Inverted-L- and T-Shaped Parasitic Elements," in *IEEE Antennas and Wireless Propagation Letters*, vol. 12, pp. 1299-1302, 2013. DOI: 10.1109/LAWP.2013.2283796

[12] R. S. Aziz, M. A. S. Alkanhal, and A.-F. Sheta, "Multiband Fractal-Like Antennas," *Progress In Electromagnetics Research B*, Vol. 29, 339-354, 2011. DOI:10.2528/PIERB11030904.

[13] Gupta, A., Joshi, H., & Khanna, R. (2017). An X-shaped fractal antenna with DGS for multiband applications. International Journal of Microwave and Wireless Technologies, 9(5), 1075-1083. DOI:10.1017/S1759078716000994.

[14]Sreelakshmi, K., Rao, G.S. Reconfigurable Quad-Band Antenna for Wireless Communication. J. Electr. Eng. Technol. 15, 2239–2249 (2020). https://doi.org/10.1007/s42835-020-00492-9